Received: 7 February 2025 | Revised: 3 April 2025 | Accepted: 7 April 2025

DOI: 10.1002/alz.70231

Alzheimer's & Dementia®
THE JOURNAL OF THE ALZHEIMER'S ASSOCIATION

RESEARCH ARTICLE

PLCG2 modulates TREM2 expression and signaling in response to Alzheimer's disease pathology

Evan J. Messenger[1] | Sydney A. Baar[1] | Logan M. Bedford[1] | Andy P. Tsai[1] | Peter Bor-Chian Lin[1] | Chloe A. Ferguson[1] | Guixiang Xu[1] | Abigail Wallace[1] | Gary E. Landreth[1,2] | Bruce T. Lamb[1,3] | Stephanie J. Bissel[1,3]

[1]Stark Neuroscience, Indiana University School of Medicine, Indianapolis, Indiana, USA

[2]Department of Anatomy, Cell Biology & Physiology, Indiana University School of Medicine, Indianapolis, Indiana, USA

[3]Department of Medical and Molecular Genetics, Indiana University School of Medicine, Indianapolis, Indiana, USA

Correspondence
Bruce T. Lamb and Stephanie J. Bissel, Stark Neuroscience, Indiana University School of Medicine, 320 W 15th Street 414C, Indianapolis, IN 46202, USA.
Email: btlamb@iu.edu, sbissel@iu.edu

Funding information
IU/JAX/PITT MODEL-AD Center, Grant/Award Number: U54AG054345; IU/Purdue TREAT-AD Center, Grant/Award Number: U54AG065181; NIA Training Grant on Alzheimer's Disease and ADRD at Indiana University, Grant/Award Number: T32AG071444; Paul and Carole Stark Medical Neuroscience Fellowship; National Institute on Aging, Grant/Award Number: RF1AG074566

Abstract

BACKGROUND: Phospholipase C gamma 2 (PLCG2) is an intracellular effector of microglial cell surface receptors, including triggering receptor expressed on myeloid cells 2 (TREM2). Variants which alter PLCG2 activity impact Alzheimer's disease (AD) risk, but the effects of PLCG2 deficiency in AD remain unclear.

METHODS: 5xFAD mice were crossed with PLCG2- and TREM2-deficient mice to assess the role of PLCG2 in response to amyloid pathology. Human bulk RNA-sequencing data were used to validate findings in AD patients.

RESULTS: In 5xFAD mice, the absence of PLCG2 resulted in reduced TREM2 expression and impaired microglial associations with amyloid beta plaques. Transcriptomic analysis revealed perturbations in immune-related pathways shared between PLCG2 and TREM2 deficiencies, as well as distinct differences. Human transcriptomics revealed positive correlations between *PLCG2* and *TREM2* independent of pathological scores.

DISCUSSION: PLCG2 is a critical component of TREM2 signal transduction and may play an upstream role in TREM2 regulation. These findings clarify the mechanisms of risk and protective PLCG2 variants.

KEYWORDS
5xFAD, Alzheimer's disease, amyloid pathology, immune response, microglia, phospholipase C gamma 2, triggering receptor expressed on myeloid cells 2

Highlights

- The role of phospholipase C gamma 2 (PLCG2) deficiency in response to amyloid beta (Aβ) pathology was investigated in 5xFAD mice and with human cortical transcriptomics.
- PLCG2 deficiency significantly reduces triggering receptor expressed on myeloid cells 2 (TREM2) expression, while TREM2 deficiency increases PLCG2 expression.

- *PLCG2* expression predicts *TREM2* expression in human cortex independent of pathology.
- PLCG2 and TREM2 deficiencies similarly impair microglial responses to Aβ plaques, exacerbate neuronal pathology, and impair gene expression associated with immune responses.
- PLCG2 deficiency confers distinct transcriptional perturbations from TREM2 deficiency.
- PLCG2 may play an upstream role in the regulation of the TREM2-mediated immune response.

1 | BACKGROUND

Alzheimer's disease (AD) is a devastating neurodegenerative disorder affecting > 55 million people worldwide.[1] AD is characterized by extracellular deposition of amyloid beta (Aβ), intraneuronal accumulation of neurofibrillary tangles (NFTs), and eventual neuronal death and cognitive decline.[2–4] Microglia, the innate immune cells of the brain, dynamically interact with these disease processes to influence AD progression.[5] Recently, advances in sequencing technology and large-scale genome-wide association studies have facilitated the discovery of rare gene variants that confer altered AD risk.[6–8] A significant proportion of these AD-linked genes are associated with microglia and the immune response, reinforcing the necessity to understand the intersection of immunity and AD pathogenesis in the development of novel AD therapeutics.[6–9]

Notably, emerging among these genes associated with AD risk is phospholipase C gamma 2 (PLCG2). PLCG2 is expressed principally by immune cells, including myeloid lineage cells, B cells, and other lymphocytes, and in the brain is inducibly expressed by plaque-associated microglia.[10–12] Upon tyrosine phosphorylation by upstream receptor complexes, PLCG2 undergoes an activating conformational change and is recruited to the plasma membrane. At the membrane, it hydrolyzes the lipid phosphatidylinositol (4,5)-bisphosphate (PIP_2) into the second messengers inositol (1,4,5)-trisphosphate (IP_3) and diacylglycerol (DAG).[13,14] PLCG2 plays a critical role in transducing signals emanating from a number of immune receptors, acting as an intracellular hub for immune signaling.[15–21]

Genetic variants of PLCG2 are associated with altered risk for AD, and mutations which alter its function result in pleiotropic effects impacting immune, vascular, and nervous functions, as well as contributing to cancer pathogenesis and treatment resistance.[10,11] Interestingly, in the brain, there exists a remarkably tight window whereby a modest increase in enzymatic activity is associated with protective effects while reduced or robust increases in activity prove detrimental.[13,14] With respect to AD, the mildly hypermorphic $PLCG2^{P522R}$ variant is associated with increased longevity, improved clearance of Aβ, and protection against AD.[22–27] Conversely, the loss-of-function $PLCG2^{M28L}$ variant confers resistance to the Bruton Tyrosine Kinase inhibitor ibrutinib, worsens Aβ pathology, and increases risk of AD.[27–29] Similarly, studies of *PLCG2* haploinsufficiency in mice have revealed that reduced PLCG2 expression impairs expression of inflammation-associated genes.[12] Surprisingly, recent studies have identified a role for gene dosage in microglial genes, including *TREM2*, whereby partial and complete loss of gene expression resulted in divergent phenotypic consequences, emphasizing the importance of exploring total PLCG2 loss.[30,31] Elucidating the effects of total PLCG2 loss in an AD mouse model will allow for the discrimination of mechanisms arising from PLCG2 enzymatic activity, microglial topology, and effects on its associated signaling complexes. Moreover, it will reveal mechanisms relevant in imparting the beneficial and detrimental effects of $PLCG2^{P522R}$ and $PLCG2^{M28L}$ variants, respectively.

There has been recent interest in uncovering the intracellular elements that mediate and coordinate neuroprotective functions of microglia downstream of immune receptors in vivo, especially triggering receptor expressed on myeloid cells 2 (TREM2).[17,32–35] TREM2 plays a key and enigmatic role in the progression of AD, acting to drive microglial phagocytosis, survival, lipid homeostasis, and metabolism.[15,36–41] Murine microglia lacking TREM2 have deficient responses to Aβ and impaired acquisition of the neuroprotective disease-associated microglia (DAM) phenotype.[39,41,42] Importantly, PLCG2-deficient human induced pluripotent stem cell (iPSC)–derived microglia (iMG) phenocopy the impaired survival and phagocytosis of myelin observed in TREM2-deficient iMG.[16] Additionally, PLCG2 has a non-redundant role in regulating calcium flux downstream of TREM2.[43] This evidence emphatically reinforces the importance of PLCG2 as a mediator of TREM2 signal transduction and the necessity of exploring this pathway in depth. Subsequently, we sought to dissect the functional and transcriptomic effects mediated by total PLCG2 and TREM2 deficiencies in the 5xFAD amyloidogenic model of AD.

2 | METHODS

2.1 | Animals

5xFAD mice on the C57BL/6J background were purchased from the Jackson Laboratory (MMRRC Strain #034848-JAX). PLCG2-deficient mice (RRID: IMSR_JAX:029910) were generated as previ-

ously described.[12] Despite extensive breeding attempts of PLCG2$^{+/-}$ mice with 5xFAD$^{+/-}$ mice, we have encountered difficulty generating 5xFAD mice with total PLCG2 deficiency. At the present time, we have only acquired six 5xFAD;homozygous PLCG2 knockout mice (*Plcg2*$^{-/-}$). While we did not observe overt changes in expected litter sizes, it is unclear what might be driving the non-Mendelian inheritance patterns of PLCG2-deficient mice. In different models of PLCG2 depletion, homozygous knockout embryos were found to have significant subcutaneous hemorrhaging, suggesting impacted vascular development and bleeding that may underlie embryonic death and reduced frequencies at weaning.[19,44] Previous studies have also identified significantly reduced birth rates of mice deficient in PLCG2, with females being more significantly impacted.[45] However, the mechanisms underlying any sex effects on lethality are unknown. TREM2-deficient mice (RRID: IMSR_JAX:027197) were purchased from the Jackson Laboratory and were created via an non-homologous end joining–generated 175bp deletion that introduces a stop codon at amino acid 17. These mice were crossed to 5xFAD mice to generate 5xFAD$^{Trem2-/-}$ mice.

All experiments were conducted after approval by the institutional animal care and use committee at Indiana University. The mice were housed under a controlled 12/12 hour light/dark cycle with access to food (Purina Lab Diet, 5K52) and water ad libitum. Male and female mice were included in all experimental groups. Mice were anesthetized using 1.2% 2,2,2-tribromoethanol (Avertin) and perfused with ice-cold phosphate buffered saline (PBS).

2.2 | Human *post mortem* bulk RNA-sequencing analysis

The Mount Sinai Brain Bank (MSBB) bulk RNA-sequencing (RNA-seq) data were acquired from the AD Knowledge Portal (https://adknowledgeportal.synapse.org/) and downloaded via Synapse (www.synapse.org/). The following SynIDs were downloaded: syn16795940, syn16795937, syn16795934, and syn16795931. Metadata for individuals and biospecimens were sourced from syn6101474 and syn21893059. Cohort information, transcriptomic data generation, and data preprocessing are detailed in Wang et al.[46] The MSBB bulk RNA-seq data were collected from Brodmann areas 10, 22, 36, and 44. Clinical Dementia Rating (CDR) scores were categorized into healthy control (HC, CDR = 0), mild cognitive impairment (MCI, CDR = 0.5), and AD (CDR > 0.5). The "lm" function of the "stats" package (version 4.3.3) in R was used for linear regression analyses.

2.3 | Immunofluorescence

Perfused right hemibrains from 7.5-month-old mice were fixed in 4% paraformaldehyde overnight at 4°C before being transferred to a 30% sucrose solution. Brains were then frozen and sectioned into 30-µm free-floating sections on a microtome. Three matched brain sections were immunostained for each animal. For immunostaining, free-floating sections were washed and permeabilized in 0.1% Triton X-100 in PBS (PBST) three times, followed by antigen retrieval with 1x Rodent Decloaker (Biocare Medical, RD913) at 85°C for 10 minutes. Sections were then blocked in 5% normal donkey serum in PBST for 1 hour at room temperature (RT). After blocking, the sections were incubated overnight at 4°C in 5% normal donkey serum in PBST with the following primary antibodies: rabbit anti-Iba1 (1:1000, Wako, #019-19741), sheep anti-TREM2 (1:500, R&D Systems, #AF1729), goat anti-Iba1 (1:1000; Novus Biologicals, NB100-1028), rat anti-LAMP1 (1:1000; Abcam, Ab25245), rabbit anti-CD68 (1:1000; Abcam, Ab283654); mouse anti-MOAB2 (1:1000; Novus Biologicals, NBP2-13075). After incubating overnight, the sections were washed three times in PBST and incubated for 1 hour at RT with the appropriate species-specific secondary antibodies conjugated with AlexaFluor in 5% normal donkey serum in PBST (1:1000, Invitrogen). After incubation, tissues were washed three times in PBST, mounted onto slides, and dried at RT. After drying, the slides were stained with X34 (Millipore Sigma, SML1954) by first rehydrating in PBST and then incubating with X34 (100 µM) in Coplin jars for 10 minutes at RT. Slides were then washed in X34 buffer (40% ethanol in distilled water) for 10 minutes, distilled water for 10 minutes, and PBST for 5 minutes. Last, slides were dried and cover-slipped using Prolong Gold Antifade Mountant

RESEARCH IN CONTEXT

1. **Systematic review**: The authors conducted a thorough literature review through PubMed. Existing knowledge identifies phospholipase C gamma 2 (PLCG2) as a critical component of neuroimmune signaling that impacts Alzheimer's disease (AD) risk. PLCG2 variants (PLCG2^{P522R} and PLCG2^{M28L}) have opposing effects on amyloid pathology and microglial responses in AD, but the impact of total PLCG2 deficiency on amyloid pathology has not been explored.
2. **Interpretation**: Our results show that PLCG2 may be critical for microglial triggering receptor expressed on myeloid cells 2 (TREM2) induction in the 5xFAD amyloidogenic mouse model. In human brain tissue, *PLCG2* and *TREM2* expression are positively correlated, regardless of pathological severity. PLCG2 deficiency impacts microglial reactivity to amyloid plaques, exacerbates neuropathology, and augments immune response genes similarly to TREM2 deficiency. Yet, PLCG2 deficiency confers its own distinct transcriptional changes apart from TREM2 deficiency.
3. **Future directions**: Our findings suggest an important relationship between PLCG2 and TREM2 in the response to AD pathology. Further research is necessary to interrogate this interplay and its significance to the effects of pathological and beneficial PLCG2 variants. Beyond TREM2, future studies are also merited to discover the importance of other upstream receptors of PLCG2 that are important in the microglial response to AD pathology.

(Thermo Fisher Scientific, P36930). Images were acquired on a Leica DM6 microscope or a Nikon A1R confocal microscope using similar exposure and gains and were analyzed using ImageJ software (National Institutes of Health [NIH], version 1.54j). Plaque morphology, distribution, and size were analyzed as described previously.[41,47] TREM2 immunohistochemistry was assessed qualitatively.

2.4 | Immunoblotting

Perfused left hemibrains were dissected into cortex and hippocampus and flash frozen. Six hundred µl of M-PER Mammalian Protein Extraction Reagent (Thermo Fisher Scientific, 78501) with protease and phosphatase inhibitors were added to dissected cortices prior to mechanical homogenization. Brain lysates were centrifuged at 15,000 × g for 10 minutes, and supernatants were collected and sonicated. Protein concentrations were measured using the bicinchoninic acid (BCA) Protein Assay Kit (Thermo Fisher Scientific, 23225). Protein was diluted in NuPage LDS Sample Buffer (Thermo Fisher Scientific, NP0007) and Bolt Sample Reducing Agent (Thermo Fisher Scientific, B0009) and denatured via boiling at 100°C for 10 minutes. Cortical samples (25 or 30 µg protein/sample) were used for electrophoresis with Bolt Bis-Tris Plus Mini Protein Gels, 4% to 12% (Invitrogen, NW04122BOX). Protein was transferred to polyvinylidene fluoride membranes at 400 mA. After transfer, membranes were washed in 0.1% Tween-20 in TBS (TBST) and blocked in 5% bovine serum albumin (BSA) in TBST. After blocking, the membranes were incubated overnight at 4°C in 5% BSA in TBST with the following primary antibodies: rabbit anti-PLCG2 (1:500; Cell Signaling, #3872), sheep anti-TREM2 (1:500, R&D Systems, #AF1729), mouse anti-β-actin (1:5000; Santa Cruz Biotechnology, sc-47778), rabbit anti-CD11c (1:1000; Cell Signaling, 97585S), mouse anti-IL4R alpha (1:250; R&D Systems, MAB530), mouse anti-GAPDH (1:5000; Santa Cruz Biotechnology, sc-32233). After incubation with primary antibodies, membranes were washed with TBST and incubated with horseradish peroxidase (HRP) conjugated secondary antibodies at 1:10000 in 5% BSA in TBST at RT for 1 hour, washed with TBST, developed in enhanced chemiluminescence solution, and imaged. Images were analyzed using ImageJ software.

2.5 | RNA isolation and quantitative polymerase chain reaction

Brain regions were dissected and processed as described above. Brain lysates were combined with an equal volume of RNA STAT-60 (Tel-Test Inc., CS-502) and RNA was immediately isolated using the PureLink RNA mini kit (Invitrogen, 12183020) per the manufacturer's instructions. PureLink DNase (Invitrogen, 12185010) was used for DNA clean-up following the manufacturer's recommendations. For quantitative polymerase chain reaction (qPCR), cDNA was synthesized from the isolated RNA using the High-Capacity of RNA-to-cDNA kit (Applied Biosystems). qPCR was performed using the StepOne Plus Real Time PCR system (Applied Biosystems) with Taqman Gene Expression Assays (Applied Biosystems) for *PLCG2* and *TREM2*. Relative gene expression was assessed relative to *Gapdh* and graphed as fold change in expression from wild-type levels. The relative delta Ct method was used for statistical comparisons.

2.6 | Bulk RNA-seq

Libraries of RNA samples with at least RIN 8 were prepared using KAPA mRNA Hyperprep Kit. Paired-end RNA sequencing (100 bp) with ≈ 100 million reads coverage was performed on an Illumina NovaSeq 6000 instrument. FASTQ files were aligned to the reference mouse genome mm10 with UCSC refGene annotation using STAR (v.2.7.10a), and gene read counts were generated using featureCounts (v. 2.0.3).[48–51] Sex-based batch effects were corrected for by omitting genes expressed on chromosomes X and Y. Differential gene analysis was conducted using edgeR (3.38.4).[52] Differentially expressed genes (DEG) were defined as false discovery rate (FDR)-adjusted p value ≤ 0.05 and an absolute log2foldchange ≥ 0.6. Enrichment analysis of the DEGs were conducted using DAVID[53,54] and enrichments were considered to be significant if adjusted p value ≤ 0.05. Cluster analysis, heatmap creation, and principal component analysis (PCA) were done with ClustVis.[55] Raw and processed data have been deposited to Gene Expression Omnibus (GEO; accession number GSE291648).

2.7 | Statistical analysis

Data were expressed as the mean ± standard error of the mean. Statistical analyses were performed using GraphPad Prism (GraphPad Software, version 10.2.2). Analyses were performed using Student t test or a non-parametric one-way analysis of variance with Tukey post hoc test. $P < 0.05$ was considered significant.

3 | RESULTS

3.1 | PLCG2 deficiency impairs the TREM2-dependent response to amyloid pathology

In neurodegenerative disease, microglia undergo context-dependent transcriptional reprogramming based on brain region, age, and pathology. AD pathology promotes TREM2-dependent microglial programs that are thought to be neuroprotective.[39] Because PLCG2 is a vital component of TREM2 signaling, we first evaluated the impact of PLCG2 depletion on TREM2 expression in response to amyloid pathology. The amyloidogenic 5xFAD mouse model begins accumulating amyloid as early as 2 months of age and, by 4 months of age, will begin showing behavioral impairments.[56,57] We examined 5xFAD mice at 7.5 months of age, a time point with robust amyloid pathology and behavioral deficits.[56,57] In the cortices of 5xFAD^{WT} mice, PLCG2 protein expression assessed by immunohistochemistry and immunoblotting was unchanged and TREM2 protein expression was significantly increased compared to B6^{WT} mice (Figure 1A–D). PLCG2 protein

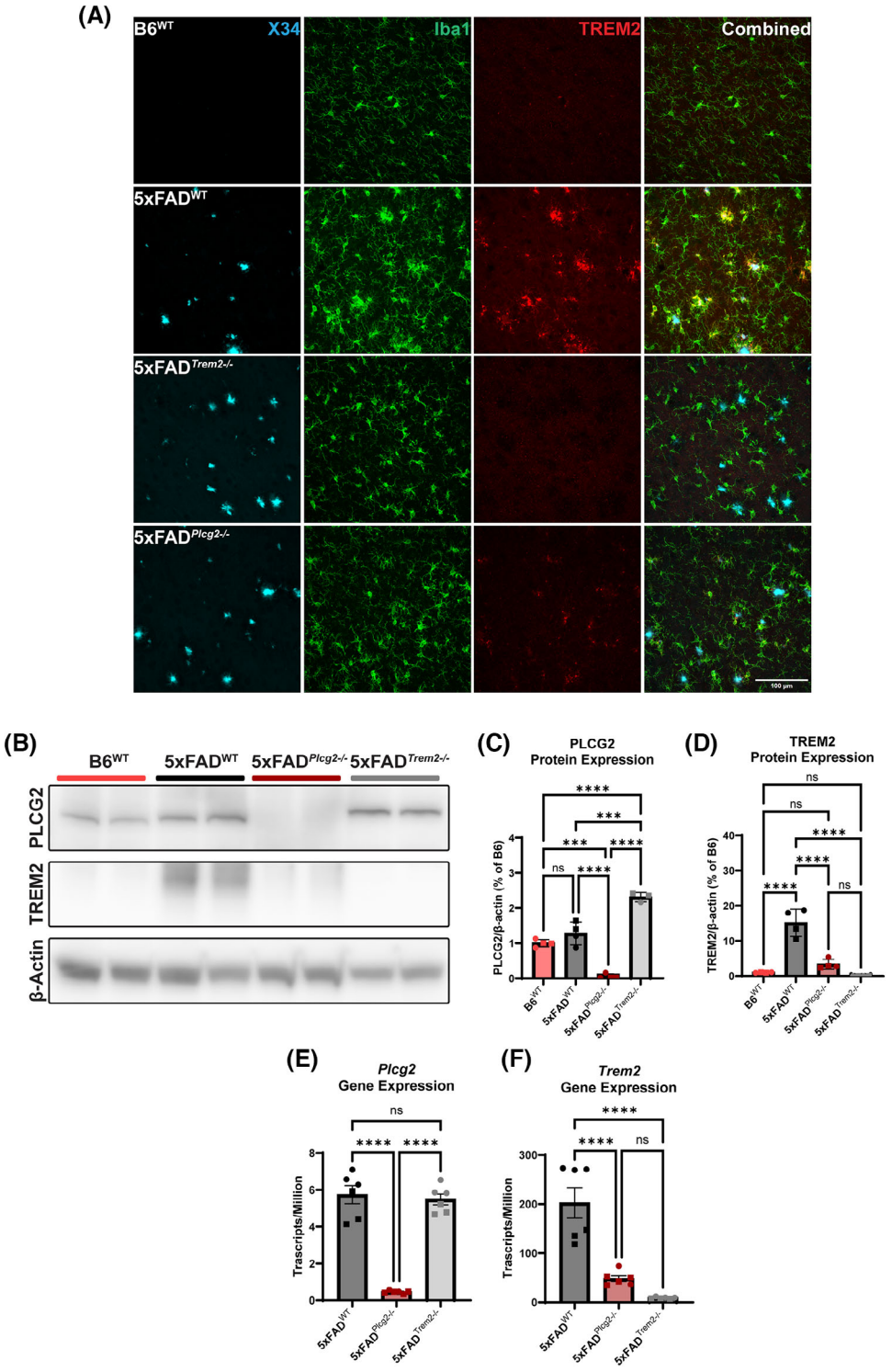

FIGURE 1 PLCG2 deficiency results in reduced *TREM2* mRNA and protein expression in 5xFAD mice. A, Representative images of plaques (X34, blue), microglia (Iba1, green), and TREM2 (red) for qualitative assessment in the cortices of 7.5-month-old mice. Scale bar, 100 µm. Representative immunoblot (B) and quantification (C and D) of PLCG2 and TREM2 protein expression in the cortices of 7.5-month-old $B6^{WT}$, $5xFAD^{WT}$, $5xFAD^{Plcg2-/-}$, and $5xFAD^{Trem2-/-}$ mice ($n = 4$ per group; 2 male and 2 female mice; TREM2 and PLCG2 expression were normalized with β-Actin). *PLCG2* (E) and *TREM2* (F) mRNA expression reported as transcripts/million (TPM) as measured by bulk-RNA sequencing of the cortices of 7.5-month-old mice ($n = 6$ per group; 3 males and 3 females for $5xFAD^{WT}$ and $5xFAD^{Trem2-/-}$ and 4 males and 2 females for $5xFAD^{Plcg2-/-}$). Male mice are marked with a square (□), and female mice are marked with a circle (°). All data are presented as the mean ± standard error of the mean analyzed by analysis of variance followed by Tukey multiple comparisons test. $^{*}p < 0.05$; $^{**}p < 0.01$; $^{***}p < 0.001$. ns, not significant; PLCG2, phospholipase C gamma 2; TREM2, triggering receptor expressed on myeloid cells 2.

expression was appropriately ablated in 5xFAD$^{Plcg2-/-}$ mice, and PLCG2 expression was increased in 5xFAD$^{Trem2-/-}$ mice compared to 5xFAD^{WT} and B6^{WT} mice (Figure 1C). Interestingly, TREM2 protein expression failed to increase in 5xFAD$^{Plcg2-/-}$ mice, despite the continued presence of microglia and Aβ plaques (Figure 1D). Similarly, mRNA expression analysis showed that while *PLCG2* expression in 5xFAD$^{Trem2-/-}$ mice was comparable to 5xFAD^{WT} mice (Figure 1E), *TREM2* mRNA expression was significantly reduced in 5xFAD$^{Plcg2-/-}$ mice compared to 5xFAD^{WT} mice (Figure 1F). Importantly, in cortices of B6$^{Plcg2-/-}$ mice, *TREM2* expression was not significantly reduced compared to B6^{WT} mice, suggesting that the observed effects of PLCG2 deficiency on *TREM2* expression might depend on the magnitude of pathology (Figure S1A,B in supporting information). Overall, these findings indicate that PLCG2 is required for induction of TREM2 in the microglial response to Aβ plaques.

3.2 | *PLCG2* expression correlates with *TREM2* expression independently of AD pathology in human bulk RNA-seq

Previously, *PLCG2* expression was shown to be associated with Aβ plaque load and the microglia markers *AIF1* and *TMEM119* in human brains.[12] To assess whether the relationship we observed between *PLCG2* and *TREM2* in 5xFAD mice translates to human brains, we used bulk RNA-seq data collected by the MSBB study. In addition to gene expression data across multiple brain regions, this study has compiled clinical and neuropathological scores for > 200 patients, including Braak staging, CDR, and the Consortium to Establish a Registry for Alzheimer's Disease (CERAD) score.[46] In four different brain regions, simple linear regression analyses were used to test if *PLCG2* expression levels could predict the expression of *TREM2*. Indeed, we revealed moderate to strong correlations between *PLCG2* and *TREM2* expression levels in nearly all brain regions surveyed regardless of pathological scoring (Figure 2A–C). Moreover, because both *PLCG2* and *TREM2* are predominantly expressed by microglia, we normalized their gene expression by *AIF1* expression levels to account for differing levels of microgliosis (Figure 2D). The correlations between *PLCG2* and *TREM2* expression levels remained significant in nearly all regions and pathologies after *AIF1* normalization (Figure 2E). Overall, these findings indicate that *PLCG2* expression levels significantly predict *TREM2* expression levels regardless of pathological score, suggesting that the role of *PLCG2* in regulating *TREM2* is innate to microglia function, independent of the extent of neuropathology and degree of microgliosis.

3.3 | PLCG2 and TREM2 knockouts similarly exacerbate amyloid pathology and impair microglial engagement with plaques

We next analyzed the effects that PLCG2 or TREM2 deficiency have on AD pathology. TREM2 deletion reduces microglial survival and phagocytosis in vitro and impacts plaque pathology across disease progression in amyloidogenic mouse models.[39,41,42] Moreover, the loss-of-function TREM2 variant R47H impairs microglial responses to Aβ and confers increased risk for AD.[36,38] In the cortices of 5xFAD mice, TREM2 and PLCG2 deficiencies were associated with an increase in average X34+ plaque size, but total X34+ area coverage did not reach significance, potentially due to large sex effects on plaque deposition (Figure 3A–C, Figure S2A in supporting information). However, using high-resolution microscopy and previously defined methods,[41,47] we identified changes to the distribution of X34+ plaque sizes (Figure S2B) and morphologies (Figure S2C), suggesting that TREM2 and PLCG2 deficiencies alter plaque development and compaction. Moreover, lysosomal-associated membrane protein 1 (LAMP1)-positive dystrophic neurite area normalized to the number of X34+ plaques was increased with TREM2 and PLCG2 deficiencies, although this was only significant in TREM2-deficient animals (Figure 3A,D, and E). Furthermore, we assessed MOAB2+ plaque characteristics, including area coverage, size, and degree of colocalization with X34+ plaques. Interestingly, despite increased neuritic dystrophy, PLCG2 and TREM2 knockout mice showed smaller average MOAB2+ plaque sizes compared to 5xFAD^{WT} mice, potentially suggesting impaired plaque compaction and increased diffusivity of oligomeric Aβ (Figure S3A in supporting information). These findings were corroborated with our assessment of the ratios of X34- and MOAB2-expressing plaques, whereby PLCG2 and TREM2 deficiencies resulted in larger proportions of X34 colocalization with MOAB2 compared to 5xFAD^{WT} mice (Figure S3B,C).

We next investigated microglial responses to Aβ using high-resolution confocal microscopy. We analyzed microglia (IBA1, green) and amyloid plaques (X34, blue) in the cortices of 5xFAD mice (Figure 3F). Microglia area coverage was similarly reduced by both TREM2 and PLCG2 deficiency, suggesting absent or impaired microgliosis in response to plaque pathology (Figure 3G). Plaque engagement was assessed by IBA1 and X34 colocalization, as well as IBA1 area coverage in a 50 µm-diameter circle centered on each plaque (periplaque IBA1; Figure 3H–K). TREM2 and PLCG2 deficiency similarly impaired microglial engagement with plaques. As a node acting downstream of TREM2, the microglial deficits conferred by PLCG2 depletion may be due to its impacts on TREM2 induction or signal transduction. Overall, these findings show that the microglial response to Aβ depends on both TREM2 and PLCG2.

3.4 | PLCG2 and TREM2 knockout similarly impair microglial immune pathways

Bulk RNA-seq of 7.5-month-old 5xFAD^{WT}, 5xFAD$^{Trem2-/-}$, and 5xFAD$^{Plcg2-/-}$ cortices was conducted to identify how depletion of these genes impacts gene expression and transcriptional pathways under significant plaque burden. Differential expression analysis of the bulk RNA-seq data identified 1256 DEGs ($p < 0.05$ and logFC > |0.6|) for 5xFAD$^{Plcg2-/-}$ versus 5xFAD^{WT} (Figure 4A) and 1002 DEGs for 5xFAD$^{Trem2-/-}$ versus 5xFAD^{WT} (Figure 4B). Enrichment analysis of Gene Ontology (GO) biological processes identified many pathways

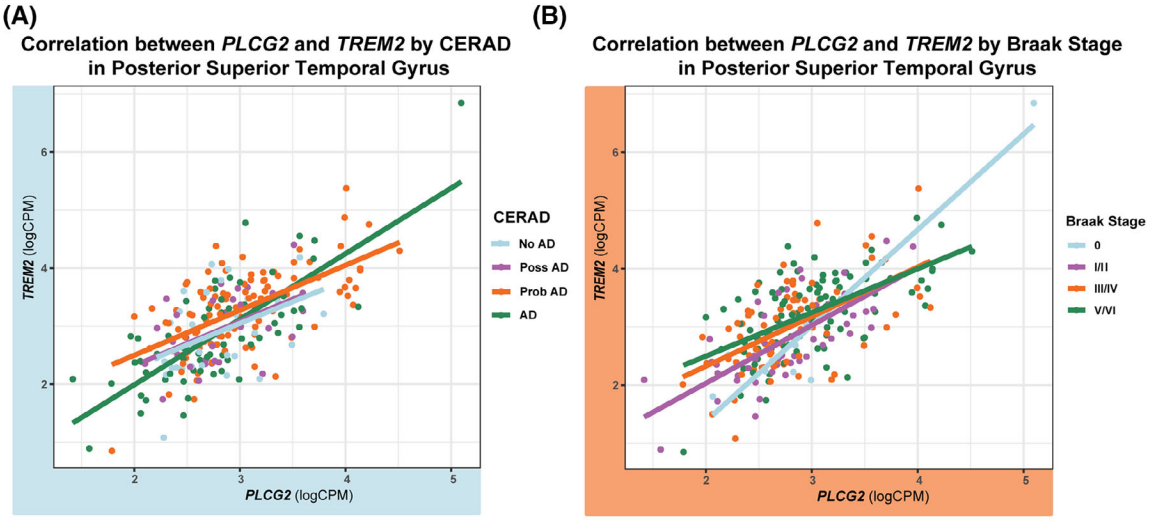

(C)

		Brodmann 10 Frontal Pole				Brodmann 22 superior temporal gyrus				Brodmann 36 parahippocampal gyrus				Brodmann 44 inferior frontal gyrus			
		R^2	P value	β	N	R^2	P value	β	N	R^2	P value	β	N	R^2	P value	β	N
CERAD Score	No AD	0.47	1.74E-06	0.37	39	0.20	5.05E-03	0.27	37	0.06	2.44E-01	0.19	26	0.48	4.06E-06	0.41	35
	AD Poss	0.26	1.81E-03	0.33	35	0.30	5.79E-04	0.39	36	0.29	1.82E-03	0.36	31	0.54	1.88E-06	0.56	32
	AD Prob	0.28	1.89E-09	0.36	111	0.37	9.39E-12	0.48	102	0.32	5.56E-09	0.48	89	0.37	2.14E-10	0.52	89
	AD	0.28	1.25E-06	0.35	75	0.58	1.76E-13	0.51	65	0.27	4.68E-06	0.35	68	0.69	1.83E-17	0.48	64
Braak Stage	0	0.81	6.20E-05	0.43	12	0.89	1.21E-04	0.54	9	0.44	5.02E-02	0.41	9	0.86	1.19E-04	0.44	10
	I/II	0.19	3.65E-04	0.34	63	0.52	1.08E-09	0.52	53	0.32	3.95E-06	0.40	57	0.64	1.15E-12	0.54	52
	III/IV	0.30	1.90E-07	0.32	79	0.34	2.00E-08	0.40	79	0.13	5.06E-03	0.27	61	0.49	3.91E-12	0.45	73
	V/VI	0.31	6.06E-10	0.39	106	0.35	1.35E-10	0.46	99	0.38	2.83E-10	0.45	87	0.40	7.78E-11	0.55	85
CDR Score	HC	0.49	2.71E-06	0.46	35	0.25	3.30E-03	0.36	33	0.02	4.64E-01	0.09	32	0.50	3.40E-05	0.41	27
	MCI	0.48	1.52E-06	0.42	38	0.64	2.71E-08	0.52	33	0.32	7.22E-04	0.41	32	0.77	1.07E-12	0.47	37
	AD	0.25	1.86E-13	0.34	187	0.39	2.00E-20	0.46	174	0.33	1.13E-14	0.44	150	0.45	1.58E-21	0.52	156

(D) $\frac{PLCG2}{AIF1}$ and $\frac{TREM2}{AIF1}$

(E)

		Brodmann 10 Frontal Pole				Brodmann 22 superior temporal gyrus				Brodmann 36 parahippocampal gyrus				Brodmann 44 inferior frontal gyrus			
		R^2	P value	β	N	R^2	P value	β	N	R^2	P value	β	N	R^2	P value	β	N
CERAD Score	No AD	0.44	4.49E-06	0.87	39	0.90	2.59E-19	2.29	37	0.37	9.26E-04	0.80	26	0.10	6.90E-02	0.96	35
	AD Poss	0.43	1.87E-05	0.94	35	0.69	3.00E-10	1.12	36	0.32	9.86E-04	0.78	31	0.48	1.23E-05	0.88	32
	AD Prob	0.64	1.32E-25	1.12	111	0.59	6.36E-21	1.23	102	0.61	1.47E-19	0.85	89	0.65	2.04E-21	0.94	89
	AD	0.35	2.50E-08	0.68	75	0.50	4.71E-11	0.94	65	0.40	8.22E-09	0.88	68	0.38	7.25E-08	0.78	64
Braak Stage	0	0.46	1.46E-02	0.67	12	0.56	1.96E-02	1.08	9	0.75	2.64E-03	0.76	9	0.12	3.29E-01	1.59	10
	I/II	0.29	5.34E-06	0.75	63	0.57	7.55E-11	0.99	53	0.40	1.11E-07	1.00	57	0.30	3.10E-05	0.71	52
	III/IV	0.34	1.33E-08	0.79	79	0.84	7.22E-32	2.14	79	0.34	7.13E-07	0.84	61	0.40	1.49E-09	0.79	73
	V/VI	0.68	1.90E-27	1.12	106	0.61	8.90E-22	1.20	99	0.58	1.58E-17	0.77	87	0.69	4.45E-23	0.93	85
CDR Score	HC	0.40	4.41E-05	0.67	35	0.39	9.58E-05	0.87	33	0.52	3.03E-06	0.96	32	0.58	3.66E-06	1.10	27
	MCI	0.21	4.12E-03	0.54	38	0.90	4.27E-17	2.26	33	0.50	6.93E-06	1.17	32	0.07	1.02E-01	0.79	37
	AD	0.60	3.05E-38	1.07	187	0.59	3.90E-35	1.14	174	0.48	8.77E-23	0.75	150	0.57	4.56E-30	0.90	156

FIGURE 2 *PLCG2* and *TREM2* correlate independently of AD pathology in human bulk RNA-sequencing. Representative scatterplot and regression lines for *PLCG2* and *TREM2* in Brodmann area 10 (posterior superior temporal gyrus) by CERAD score (A) and Braak stage (B). The table (C) shows the R^2, *p* value, *β* coefficient (*β*), and population size (*N*) of the simple linear regression analysis between *PLCG2* and *TREM2* depending on each patient's CERAD score, Braak stage, and CDR score. Blue and orange areas indicate respective linear regression statistics for representative plots (A–C). D, To account for individual differences in microgliosis, *PLCG2* and *TREM2* were divided by the microglia marker *AIF1*, and the simple linear regression analysis was repeated (E). AD, Alzheimer's disease; CERAD, Consortium to Establish a Registry for Alzheimer's Disease; CDR, Clinical Dementia Rating; PLCG2, phospholipase C gamma; TREM2, triggering receptor expressed on myeloid cells 2.

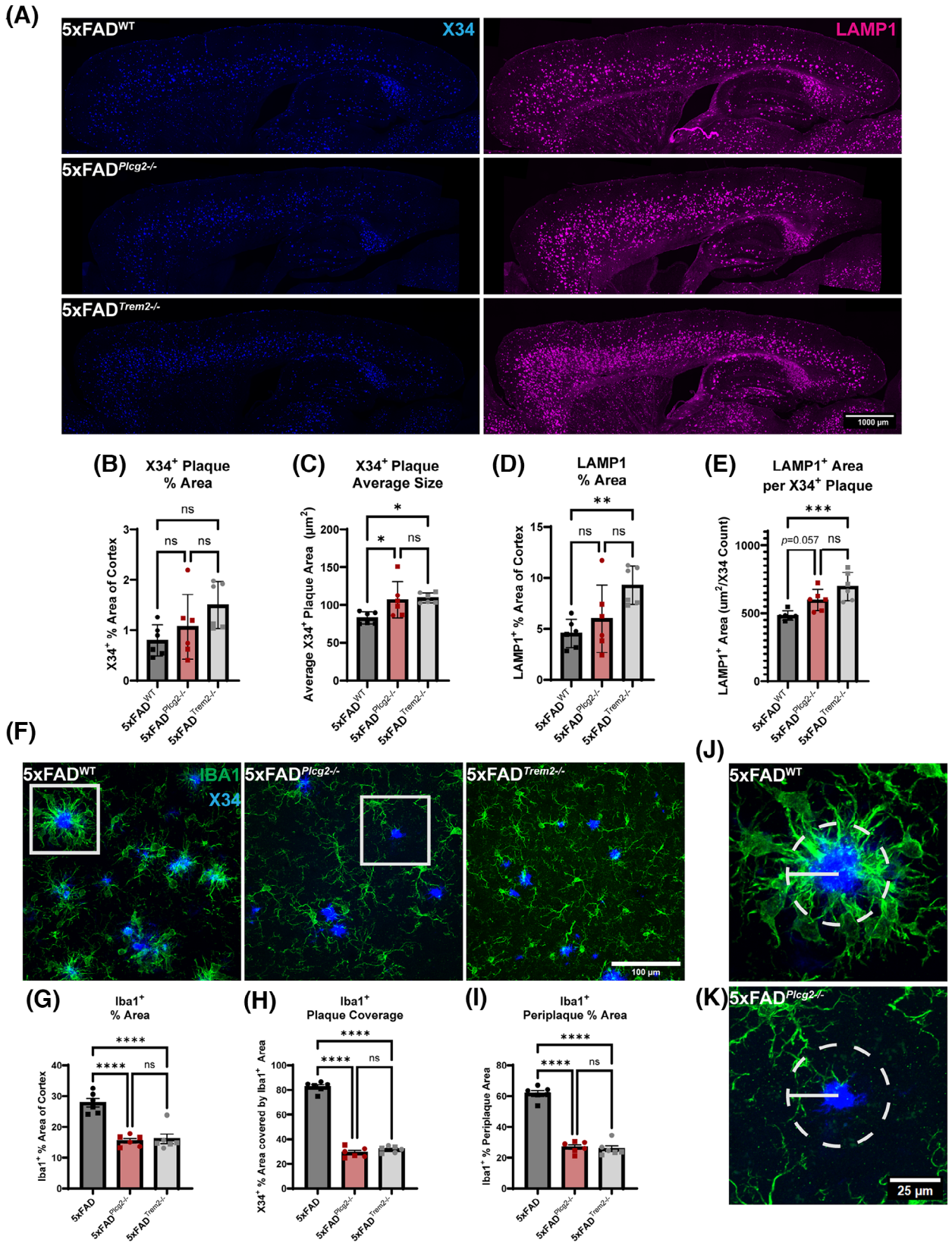

FIGURE 3 PLCG2 and TREM2 deficiency exacerbate amyloid pathology and impair microglial engagement with Aβ plaques. (A) Representative images of dense-core plaques (X34, blue) and dystrophic neurites (LAMP1, magenta) in the cortices of 7.5-month-old 5xFAD^{WT}, 5xFAD$^{Plcg2-/-}$, and 5xFAD$^{Trem2-/-}$ mice. Scale bar, 1000 µm. Percentage of X34+ area (B) or LAMP1+ area (D) in the cortices of 7.5-month-old mice of each genotype. Average X34+ plaque size (C), and LAMP1 total area per X34+ plaque (E) in the cortices of 7.5-month-old mice of each genotype. F, Representative images of dense-core plaques (X34, blue) and microglia (Iba1, green) in cortices of 7.5-month-old mice. Total percentage of Iba1+

associated with the immune response that were shared between both 5xFAD$^{Plcg2-/-}$ and 5xFAD$^{Trem2-/-}$ compared to 5xFAD^{WT}, including immune response, regulation of immune system process, and defense response (Figure 4C,D). Indeed, expression of genes related to the TREM2-mediated microglial response to Aβ, including *Itgax*, *Clec7a*, and *Cd68*, were significantly reduced in both 5xFAD$^{Plcg2-/-}$ and 5xFAD$^{Trem2-/-}$ mice compared to 5xFAD^{WT} mice (Figure 4E). Immunohistochemistry of phagolysosomal marker CD68 showed reduced immunoreactivity in both 5xFAD$^{Plcg2-/-}$ and 5xFAD$^{Trem2-/-}$ mice compared to 5xFAD^{WT} mice, corroborating the bulk RNA-seq findings (Figure 4F–G,J). Interestingly, 5xFAD$^{Plcg2-/-}$ mice showed greater reductions in CD68 immunoreactivity in IBA1+ microglia and in the periplaque regions than 5xFAD$^{Trem2-/-}$ mice (Figure 4H–I), suggesting that phagolysosomal processes rely only in part on TREM2 but more substantially on PLCG2, potentially through other receptors which depend on PLCG2-mediated signal transduction. Additionally, *Itgax*/CD11c expression is associated with pro-phagocytic phenotypes in microglia, and analysis of CD11c in 7.5-month-old 5xFAD animals using immunoblotting revealed near total depletion of protein in both 5xFAD$^{Plcg2-/-}$ and 5xFAD$^{Trem2-/-}$ mice compared to 5xFAD^{WT} mice (Figure 4K,L). These results show that PLCG2 and TREM2 deficiencies similarly impair the microglia-mediated immune response to Aβ by impacting the induction of TREM2-mediated transcriptional programs, reinforcing the importance of PLCG2 as a signaling node in the TREM2 signaling pathway.

3.5 | PLCG2 and TREM2 knockouts confer distinct transcriptional perturbations

The intracellular signaling pathway downstream TREM2 is complex and involves many molecules in addition to PLCG2, including Syk and PI3K.[32,33,35,43,58,59] Likewise, PLCG2 mediates transduction of many other cell surface receptors in addition to TREM2.[13,15–21] To clarify the role of the TREM2–PLCG2 axis among these pathways in AD, we dissected the DEGs identified by bulk RNA-seq. PCA revealed discrete clusters of each genotype (Figure 5A). These clusters showed that despite similar phenotypes in AD, 5xFAD$^{Plcg2-/-}$ and 5xFAD$^{Trem2-/-}$ mice exhibit distinct transcriptional profiles. We next analyzed shared and unshared DEGs between 5xFAD$^{Plcg2-/-}$ and 5xFAD$^{Trem2-/-}$ versus 5xFAD^{WT} to identify what pathways may be unique to the networks in which PLCG2 and TREM2 participate. There were 469 shared DEGs, 581 specific for 5xFAD$^{Plcg2-/-}$ mice, and 382 specific for 5xFAD$^{Trem2-/-}$ mice (Figure 5B, Figure S4 in supporting information). Enrichment analysis of GO biological processes for the shared DEGs revealed mostly immune response pathways, reinforcing our findings of impaired microglial functioning in response to Aβ (Figure 5C). Interestingly, analysis of 5xFAD$^{Plcg2-/-}$-specific genes showed unique pathways related to cell surface receptor signaling, migration, and cytokine production (Figure 5D), while analysis of 5xFAD$^{Trem2-/-}$-specific genes showed pathways associated with cell adhesion and development (Figure 5E). To validate these transcriptomic alterations at the protein level, we identified *Il4ra*, a gene associated with cell surface receptor transduction and interleukin 4 signaling, that was differentially expressed between PLCG2- and TREM2-deficient animals. Interestingly, we identified a potential sex- and genotype-dependent effect on *Il4ra* isoform proportions, potentially indicating an effect on alternative splicing for this gene (Figure S5A–C in supporting information). Further experiments are required to elucidate the sex- and PLCG2- and TREM2-dependent mechanisms on this pathway. These genes and associated pathways reveal insights into which mechanisms might be uniquely disrupted in each condition and will help delineate the role that PLCG2 plays as a node of many different upstream signaling sources.

4 | DISCUSSION

While *PLCG2* mutations have been most thoroughly studied in the context of peripheral inflammatory disorders, recent genetic studies have revealed genetic variants in *PLCG2* that divergently impact AD risk.[11,22–27,29] In light of the findings that the GOF P522R variant of *PLCG2* confers protection in AD and the M28L variant confers risk, it has become critical to achieve a better understanding of the mechanisms through which PLCG2 augments microglial functioning to inform the discovery of immunomodulatory therapies for AD. The role of PLCG2 in vital signal transduction pathways of microglial immune receptors, especially TREM2, remains unclear in the context of AD. Here, we identify the importance of PLCG2 in the TREM2-dependent microglial response in vivo, transcriptomic disturbances distinguishing PLCG2 and TREM2 function, and a potential upstream regulatory role of PLCG2 in the 5xFAD amyloidogenic murine model of AD.

In AD, amyloid pathology induces the expression of TREM2 in microglia.[36–41,60] Previous work has shown that PLCG2 depletion inhibits TREM2 signaling in response to TREM2 ligands in vitro.[16] Interestingly, we showed that PLCG2 deficiency completely inhibited the induction of TREM2 in plaque-associated microglia and reduced cortical gene expression to near knockout levels in 5xFAD mice. Thus, PLCG2-deficient 5xFAD animals appeared to be function-

area (G) within the cortex, total percent of X34+ plaque area colocalized with Iba1+ area (H), and percentage of periplaque Iba1+ microglia (I) within a circular area with a radius of 25 µm centered on X34^{+} plaques ($n = 6$ mice and > 100 plaques per genotype) in the cortices of 7.5-month-old mice of each genotype. J,K, Representative images illustrating periplaque regions in 5xFAD^{WT} and 5xFAD$^{Plcg2-/-}$ mice. Scale bar, 25 µm. $n = 6$ per group; 3 males and 3 females for 5xFAD^{WT} and 5xFAD$^{Trem2-/-}$ and 4 males and 2 females for 5xFAD$^{Plcg2-/-}$. Male mice are marked with a square (□), and female mice are marked with a circle (°). Data points represent means of three matched sagittal sections per mouse. All data are presented as the mean ± standard error of the mean analyzed by analysis of variance followed by Tukey multiple comparisons test. $^{*}p < 0.05$; $^{**}p < 0.01$; $^{***}p < 0.001$. Aβ, amyloid beta; LAMP1, lysosomal-associated membrane protein 1; ns, not significant; PLCG2, phospholipase C gamma; TREM2, triggering receptor expressed on myeloid cells 2.

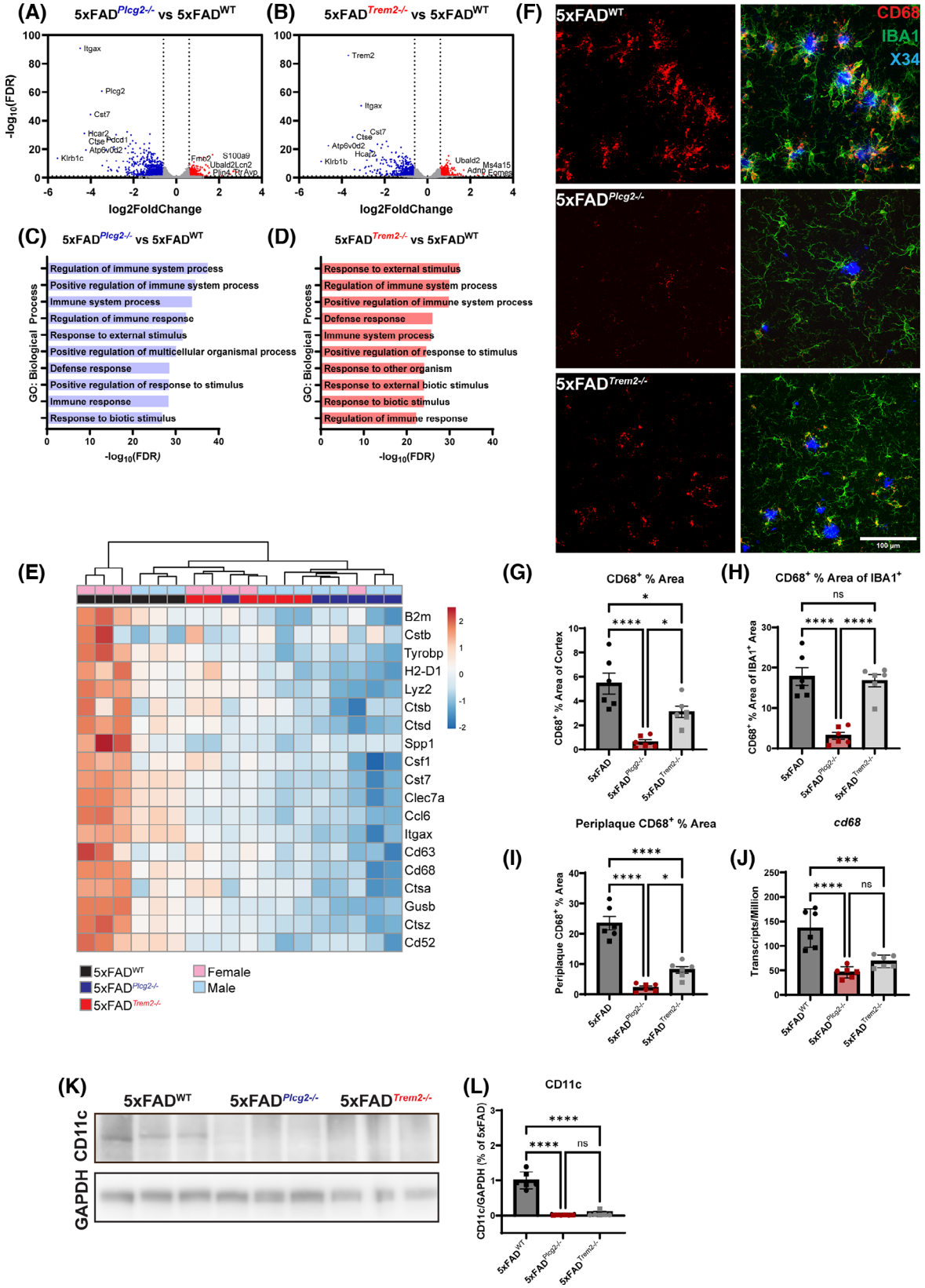

FIGURE 4 PLCG2 and TREM2 deficiency similarly impair immune pathways. Cortices of 5xFAD^{WT}, 5xFAD$^{Plcg2-/-}$, and 5xFAD$^{Trem2-/-}$ mice were harvested at 7.5 months for bulk RNA-sequencing analysis. A, Volcano plot showing significant DEGs (FDR < 0.05, FC > 1.5) between 5xFAD$^{Plcg2-/-}$ and 5xFAD^{WT} mice. B, Volcano plot showing significant DEGs (FDR < 0.05, FC > 1.5) between 5xFAD$^{Trem2-/-}$ and 5xFAD^{WT}. C, Top 10 GO terms for biological processes using all DEGs that met the significance and FC threshold between 5xFAD$^{Plcg2-/-}$ and 5xFAD^{WT} mice. D, Top 10 GO terms for biological processes using all DEGs that met the significance and FC threshold between 5xFAD$^{Trem2-/-}$ and 5xFAD^{WT} mice. E, Heatmap depicting

ally nearly TREM2 deficient, as well. These results recapitulated in vitro findings in myeloid cells by Obst et al., which showed a significant reduction in *TREM2* expression in PLCG2-deficient iPSC-derived human macrophages.[43] Moreover, in PLCG2-deficient B6 mice, *TREM2* expression was reduced, but did not reach significance, potentially due to low expression of *TREM2* in non-diseased model mice. Thus, we cannot rule out the contribution of PLCG2 deficiency during development and homeostasis to our findings. Conversely, in 5xFAD mice, we found TREM2 depletion does not affect PLCG2 gene expression. These findings strongly suggest that PLCG2 is critical for the TREM2-mediated microglial response to amyloid plaques. Furthermore, examining the human brain bulk RNA-seq data collected by the MSBB,[46] this finding was recapitulated because *PLCG2* expression significantly predicts *TREM2* expression in multiple brain regions. Importantly, these findings are irrespective of neuropathological scores, suggesting that PLCG2 plays a vital role in TREM2 regulation in both healthy aging and disease. While previous research established the importance of PLCG2 downstream of TREM2, our study suggests a novel role for PLCG2 upstream of the TREM2 response.

TREM2 loss-of-function impairs microglial protective functions and worsens neuronal dystrophy.[9,37,38,41,42,61] Likewise, PLCG2 loss-of-function has recently been associated with worsened AD pathology.[12,27,29] Indeed, we observed that both PLCG2 and TREM2 deficiencies similarly exacerbated amyloid-induced neuropathology and significantly reduced microglial coverage and engagement of plaques. However, we did identify reduced MOAB2+ plaque sizes with PLCG2 and TREM2 deficiencies despite increased neuritic plaque pathology, which may be a result of reduced oligomeric Aβ compaction as described previously in another amyloidogenic mouse model.[62] Overall, these findings agree with previous research that reported that PLCG2 deficiency phenocopies the deficits in phagocytosis and immune reactivity to stimuli resulting from TREM2 deficiency in vitro.[16,43] Of note, the effects of TREM2 depletion depend on the stage of disease progression, in which it ameliorates pathology early and exacerbates it later in the APP PS1-21 mouse model.[42] The current findings in 7.5-month-old 5xFAD mice recapitulate previous findings in later disease stages, but changes in pathology and microglial phenotypes due to PLCG2 depletion should be investigated across a greater range of ages.

Alterations in TREM2 and PLCG2 expression are associated with significant transcriptional shifts, including in pathways associated with immunity, metabolism, proliferation, and autophagy.[12,16,25,39,43] To better understand the level of signaling input TREM2 relays to PLCG2 under significant amyloid plaque burden, we conducted bulk RNA-seq on whole cortices of 7.5-month-old 5xFAD mice in TREM2-deficient and PLCG2-deficient animals and examined functional pathways. Of note, bulk RNA-seq does not allow for the assessment of cell type–specific gene expression. Although the discussed DEGs are predominantly expressed by microglia, they must be interpreted with respect to the whole brain rather than specifically microglia. Interestingly, the DEGs of both genotypes were almost entirely associated with immune-related terms. The transcriptional shift microglia undergo in response to Aβ is thought to be at least partially dependent on TREM2 expression,[33,39] and the majority of the genes associated with the TREM2-dependent microglial program are significantly downregulated in PLCG2 deficient brains, as well. Analysis of both *Itgax*/CD11c and *Cd68*, markers of microglial responsivity and phagocytosis associated with the TREM2 response to Aβ, confirmed significantly impaired induction of the TREM2-dependent genes in both PLCG2 and TREM2-deficient cortices. These findings reinforce the importance of PLCG2 in the TREM2-dependent immune response to Aβ.

PLCG2-deficient iMGs at baseline shared almost 50% of the DEGs identified in TREM2-deficient iMGs, and these genes were enriched in pathways associated with phagocytosis and DAP12 signaling,[16] illustrating the importance of PLCG2 in these canonically TREM2-associated mechanisms. Thus, we hypothesized that these transcriptional similarities would exist in vivo in amyloidogenic mouse models, as well. Our analysis revealed that of the 1256 DEGs identified for 5xFAD$^{Plcg2-/-}$ versus 5xFAD^{WT} mice and 1002 DEGs for 5xFAD$^{Trem2-/-}$ versus 5xFAD^{WT} mice, 578 were shared. Indeed, these shared DEGs were heavily enriched for immune-related pathways, supporting the role of PLCG2 in mediating TREM2-dependent microglial responses. Importantly, the PCA revealed that while PLCG2 and TREM2 deficiencies share many significant terms, they are transcriptionally distinct. This suggests that PLCG2 signaling has non-TREM2-mediated input in response to pathology. The unshared DEGs provide insight into what pathways may be uniquely affected by each knockout and can inform what other signaling mechanisms or downstream nodes participate.

Enrichment of genes specific to PLCG2 deficiency revealed pathways associated with cell surface receptor signaling, migration, proliferation, and cytokine production, recapitulating previous in vitro findings which identified reductions in integrin expression, deficits in motility, and alterations in cytokine signaling in PLCG2 deficient iPSC-macrophages, iMGs, and neutrophils.[16,18,43] Additionally, these results bolster our understanding of PLCG2 as a node of many receptors with numerous downstream consequences of activation. Despite these transcriptomic differences, however, PLCG2 and TREM2 deficiencies exhibited similar microglial phenotypes, amyloid plaque burden, and

mRNA expression of disease-associated microglia genes between 5xFAD^{WT}, 5xFAD$^{Plcg2-/-}$, and 5xFAD$^{Trem2-/-}$ mice. F, Representative images of dense-core plaques (X34, blue), microglia, (Iba1, green), and phagolysosomes (CD68, red). Scale bar, 100 µm. G, Total percentage of CD68^{+} area. H, Total percentage of CD68 area normalized to total Iba1^{+} area. I, Percentage of periplaque CD68^{+} area within a circular area with a radius of 25 µm centered on X34^{+} plaques. J, *CD68* mRNA expression reported as transcripts/million (TPM). Representative immunoblot (K) and quantification (L) of CD11c protein from in 5xFAD^{WT}, 5xFAD$^{Plcg2-/-}$, and 5xFAD$^{Trem2-/-}$ cortices. Male mice are marked with a square (□), and female mice are marked with a circle (○). All data are presented as the mean ± standard error of the mean analyzed by analysis of variance followed by Tukey multiple comparisons test. *$p < 0.05$; **$p < 0.01$; ***$p < 0.001$. DEGs, differentially expressed genes; FC, fold change; FDR, false discovery rate; GO, Gene Ontology; ns, not significant; PLCG2, phospholipase C gamma; TREM2, triggering receptor expressed on myeloid cells 2.

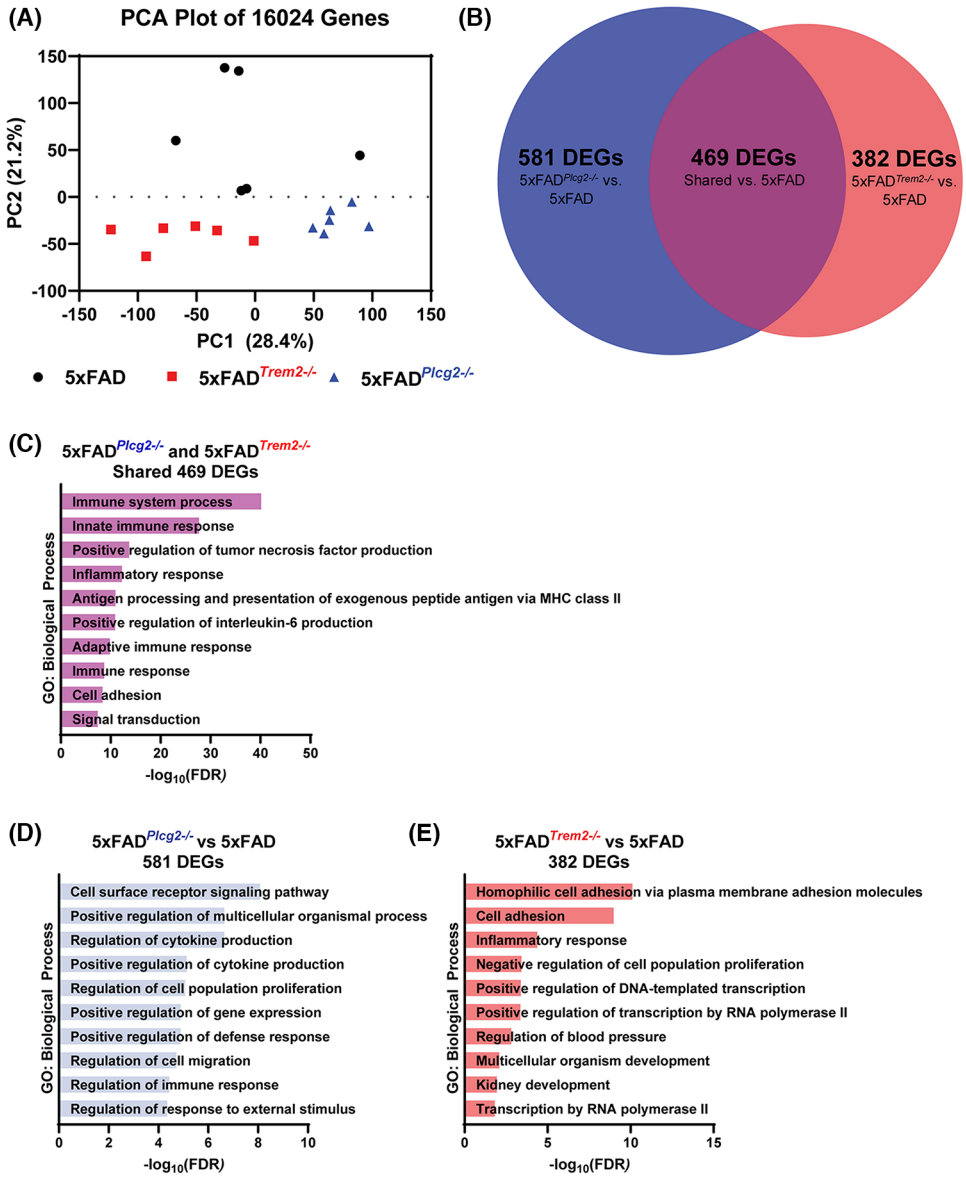

FIGURE 5 PLCG2 and TREM2-deficient 5xFAD mice share altered pathways but are transcriptionally distinct. A, PCA plot showing clustering of each genotype. B, Euler diagram showing the quantity of shared and unshared DEGs ($p < 0.05$, FC > 1.5) between 5xFAD$^{Plcg2-/-}$ versus 5xFAD^{WT} mice and 5xFAD$^{Trem2-/-}$ versus 5xFAD^{WT} mice. C–E, The top 10 GO terms for biological processes for shared DEGs (E; purple) and unshared DEGs (C; blue and D; red). DEGs, differentially expressed genes; FC, fold change; GO, Gene Ontology; PCA, principal component analysis; PLCG2, phospholipase C gamma; TREM2, triggering receptor expressed on myeloid cells 2.

neuronal dystrophy, suggesting that the pathways that are most relevant in the context of severe amyloid pathology may be those that were shared.

These results help clarify the role of PLCG2 in mediating microglial responses to Aβ and provide valuable insight into the functions of the protective and risk PLCG2 variants. Similar to total PLCG2 knockout, the loss-of-function PLCG2^{M28L} variant reduces PLCG2 expression, exacerbates AD pathology, impairs microglial responsivity to Aβ, and disrupts microglial response gene expression.[27] Through investigation of total PLCG2 loss, we show that PLCG2 may be critical for facilitating upregulation of TREM2 in response to Aβ in addition to mediating downstream transduction. Future high-powered studies should clarify how sex impacts PLCG2 and TREM2 function in AD, as well as explore the relationship between PLCG2^{M28L} and both PLCG2 and TREM2 deficiencies to further elucidate the mechanisms by which it confers risk for AD.

AUTHOR CONTRIBUTIONS

Evan J. Messenger and Stephanie J. Bissel conceived and designed the study. Evan J. Messenger conducted the experiments and analyzed all the data. Sydney A. Baar and Chloe A. Ferguson assisted with IHC and WB experiments. Andy P. Tsai, Peter Bor-Chian Lin, and Guixiang Xu assisted with tissue collection and processing. Evan J. Messenger, Logan M. Bedford, Bruce T. Lamb, Gary E. Landreth, and Stephanie J.

Bissel interpreted and discussed the results. Abigail Wallace supervised and provided critical feedback. Evan J. Messenger and Stephanie J. Bissel wrote the manuscript with revisions from Gary E. Landreth and Bruce T. Lamb. All authors reviewed and approved the manuscript.

ACKNOWLEDGMENTS

The results published here are in part based on data obtained from the AD Knowledge Portal (https://adknowledgeportal.org/). These data were generated from *post mortem* brain tissue collected through the Mount Sinai VA Medical Center Brain Bank and were provided by Dr. Eric Schadt from Mount Sinai School of Medicine. Sequencing analysis was carried out in the Center for Medical Genomics at Indiana University School of Medicine, which is partially supported by the Indiana University Grand Challenges Precision Health Initiative. This work was primarily supported by NIA grant RF1 AG074566 (Lamb, Bissel, Landreth) with additional support provided by the IU/JAX/PITT MODEL-AD Center and the IU/Purdue TREAT-AD Center (U54AG054345 and U54AG065181). Evan J. Messenger was supported by the Paul and Carole Stark Medical Neuroscience Fellowship and the NIA Training Grant on Alzheimer's Disease and ADRD at Indiana University (T32AG071444).

CONFLICT OF INTEREST STATEMENT

The authors declare no competing financial interests. Author disclosures are available in the supporting information.

CONSENT STATEMENT

No human subject materials were used in this study.

ORCID

Stephanie J. Bissel https://orcid.org/0000-0002-7376-2327

REFERENCES

1. World Health Organization. *Dementia*. World Health Organization; 2023. Available from: https://www.who.int/news-room/fact-sheets/detail/dementia
2. Kosik KS, Joachim CL, Selkoe DJ. Microtubule-associated protein tau (tau) is a major antigenic component of paired helical filaments in Alzheimer disease. *Proc Natl Acad Sci U S A*. 1986;83:4044-4048.
3. Cotman CW, Su JH. Mechanisms of neuronal death in Alzheimer's disease. *Brain Pathol*. 1996;6:493-506.
4. Glenner GG, Wong CW. Alzheimer's disease and Down's syndrome: sharing of a unique cerebrovascular amyloid fibril protein. *Biochem Biophys Res Commun*. 1984;122:1131-5.
5. Lee CYD, Landreth GE. The role of microglia in amyloid clearance from the AD brain. *J Neural Transm*. 2010;117:949-60.
6. Khani M, Gibbons E, Bras J, Guerreiro R. Challenge accepted: uncovering the role of rare genetic variants in Alzheimer's disease. *Mol Neurodegener*. 2022;17:3.
7. Kunkle BW, Grenier-Boley B, Sims R, Bis JC, Damotte V, Naj AC, et al. Genetic meta-analysis of diagnosed Alzheimer's disease identifies new risk loci and implicates Aβ, tau, immunity and lipid processing. *Nat Genet*. 2019;51:414-30.
8. Nott A, Holtman IR, Coufal NG, et al. Brain cell type–specific enhancer–promoter interactome maps and disease-risk association. *Science*. 2019;366(6469):1134-1139.
9. Karch CM, Goate AM. Alzheimer's disease risk genes and mechanisms of disease pathogenesis. *Biol Psychiatry*. 2015;77:43-51.
10. Jackson JT, Mulazzani E, Nutt SL, Masters SL. The role of PLCγ2 in immunological disorders, cancer, and neurodegeneration. *J Biol Chem*. 2021;297:100905.
11. Sims R, van der Lee SJ, Naj AC, et al. Rare coding variants in PLCG2, ABI3, and TREM2 implicate microglial-mediated innate immunity in Alzheimer's disease. *Nat Genet*. 2017;49:1373-84.
12. Tsai AP, Dong C, Lin PBC, et al. PLCG2 is associated with the inflammatory response and is induced by amyloid plaques in Alzheimer's disease. *Genome Med*. 2022;14:17.
13. Magno L, Bunney TD, Mead E, Svensson F, Bictash MN. TREM2/PLCγ2 signalling in immune cells: function, structural insight, and potential therapeutic modulation. *Mol Neurodegener*. 2021;16:22.
14. Siraliev-Perez E, Stariha JTB, Hoffmann RM, et al. Dynamics of allosteric regulation of the phospholipase C-gamma isozymes upon recruitment to membranes. *Elife*. 2022;11:e77809.
15. Aki D, Minoda Y, Yoshida H, et al. Peptidoglycan and lipopolysaccharide activate PLCγ2, leading to enhanced cytokine production in macrophages and dendritic cells. *Genes Cells*. 2008;13:199-208.
16. Andreone BJ, Przybyla L, Llapashtica C, et al. Alzheimer's-associated PLCγ2 is a signaling node required for both TREM2 function and the inflammatory response in human microglia. *Nat Neurosci*. 2020;23:927-38.
17. Hu X, Li S, Doycheva DM, et al. Rh-CSF1 attenuates neuroinflammation via the CSF1R/PLCG2/PKCε pathway in a rat model of neonatal HIE. *J Neuroinflammation*. 2020;17:182.
18. Jakus Z, Simon E, Frommhold D, Sperandio M, Mócsai A. Critical role of phospholipase Cγ2 in integrin and Fc receptor-mediated neutrophil functions and the effector phase of autoimmune arthritis. *J Exp Med*. 2009;206:577.
19. Wang D, Feng J, Wen R, et al. Phospholipase Cγ2 is essential in the functions of B cell and several Fc receptors. *Immunity*. 2000;13:25-35.
20. Wen R, Jou S-T, Chen Y, Hoffmeyer A, Wang D. Phospholipase Cγ2 is essential for specific functions of FcεR and FcγR1. *J Immunol*. 2002;169:6743-6752.
21. Xu S, Huo J, Lee K-G, Kurosaki T, Lam K-P. Phospholipase Cγ2 is critical for dectin-1-mediated Ca2+ flux and cytokine production in dendritic cells*. *J Biol Chem*. 2009;284:7038-46.
22. Claes C, England WE, Danhash EP, et al. The P522R protective variant of PLCG2 promotes the expression of antigen presentation genes by human microglia in an Alzheimer's disease mouse model. *Alzheimers Dement*. 2022;18:1765-78.
23. Diks AM, Teodosio C, de Mooij B, et al. Carriers of the p.P522R variant in PLCγ2 have a slightly more responsive immune system. *Mol Neurodegener*. 2023;18:25.
24. Kleineidam L, Chouraki V, Próchnicki T, et al. PLCG2 protective variant p.P522R modulates tau pathology and disease progression in patients with mild cognitive impairment. *Acta Neuropathol*. 2020;139:1025-1044.
25. Magno L, Lessard CB, Martins M, et al. Alzheimer's disease phospholipase C-gamma-2 (PLCG2) protective variant is a functional hypermorph. *Alzheimers Res Ther*. 2019;11:16.
26. Takalo M, Wittrahm R, Wefers B, et al. The Alzheimer's disease-associated protective Plcγ2-P522R variant promotes immune functions. *Mol Neurodegener*. 2020;15:52.
27. Tsai AP, Dong C, Lin PB-C, et al. Genetic variants of phospholipase C-γ2 alter the phenotype and function of microglia and confer differential risk for Alzheimer's disease. *Immunity*. 2023;56:2121-2136.e6.
28. Li K, Ran B, Wang Y, Liu L, Li W. PLCgamma2 impacts microglia-related effectors revealing variants and pathways important in Alzheimer's disease. *Front Cell Dev Biol*. 2022;10:999061.
29. Oblak AL, Kotredes KP, Pandey RS, et al. Plcg2M28L interacts with high fat/high sugar diet to accelerate Alzheimer's disease-relevant phenotypes in mice. *Front Aging Neurosci*. 2022;14:886575.

30. Codocedo JF, Mera-Reina C, Bor-Chian Lin P, et al. Therapeutic targeting of immunometabolism reveals a critical reliance on hexokinase 2 dosage for microglial activation and Alzheimer's progression. *Cell Rep*. 2024;43:114488.
31. Sayed FA, Telpoukhovskaia M, Kodama L, et al. Differential effects of partial and complete loss of TREM2 on microglial injury response and tauopathy. *Proc Natl Acad Sci U S A*. 2018;115:10172-7.
32. Ennerfelt H, Frost EL, Shapiro DA, et al. SYK coordinates neuroprotective microglial responses in neurodegenerative disease. *Cell*. 2022;185:4135-4152.e22.
33. Krasemann S, Madore C, Cialic R, et al. The TREM2-APOE pathway drives the transcriptional phenotype of dysfunctional microglia in neurodegenerative diseases. *Immunity*. 2017;47:566-581.e9.
34. Lin PB-C, Tsai AP-Y, Soni D, et al. INPP5D deficiency attenuates amyloid pathology in a mouse model of Alzheimer's disease. *Alzheimers Dement*. 2023;19:2528-2537.
35. Soni DM, Lin PB-C, Lee-Gosselin A, et al. Inpp5d haplodeficiency alleviates tau pathology in the PS19 mouse model of Tauopathy. *Alzheimers Dement*. 2024;20:4985-4998.
36. Cheng-Hathaway PJ, Reed-Geaghan EG, Jay TR, et al. The Trem2 R47H variant confers loss-of-function-like phenotypes in Alzheimer's disease. *Mol Neurodegener*. 2018;13:29.
37. Jay TR, von Saucken VE, Landreth GE. TREM2 in neurodegenerative diseases. *Mol Neurodegener*. 2017;12:56.
38. Jonsson T, Jonsson PV, Levey AI, et al. Variant of TREM2 associated with the risk of Alzheimer's disease. *N Engl J Med*. 2013.
39. Keren-Shaul H, Spinrad A, Weiner A, et al. A unique microglia type associated with restricting development of Alzheimer's disease. *Cell*. 2017;169:1276-90.e17.
40. Wang Y, Cella M, Mallinson K, et al. TREM2 lipid sensing sustains the microglial response in an Alzheimer's disease model. *Cell*. 2015;160:1061-1071.
41. Yuan P, Condello C, Keene CD, et al. TREM2 haplodeficiency in mice and humans impairs the microglia barrier function leading to decreased amyloid compaction and severe axonal dystrophy. *Neuron*. 2016;90:724-39.
42. Jay TR, Hirsch AM, Broihier ML, t al. Disease progression-dependent effects of TREM2 deficiency in a mouse model of Alzheimer's disease. *J Neurosci*. 2017;37:637-47.
43. Obst J, Hall-Roberts HL, Smith TB, et al. PLCγ2 regulates TREM2 signalling and integrin-mediated adhesion and migration of human iPSC-derived macrophages. *Sci Rep*. 2021;11:19842.
44. Ichise H, Ichise T, Ohtani O, Yoshida N. Phospholipase Cgamma2 is necessary for separation of blood and lymphatic vasculature in mice. *Development*. 2009;136:191-5.
45. Hopp SC, Rogers JG, Smith S, et al. Multi-omics analyses reveal novel effects of PLCgamma2 deficiency in the mouse brain. *bioRxiv*. 2023. doi: 10.1101/2023.12.06.570499
46. Wang M, Beckmann ND, Roussos P, et al. The Mount Sinai cohort of large-scale genomic, transcriptomic and proteomic data in Alzheimer's disease. *Sci Data*. 2018;5:180185.
47. Puntambekar SS, Moutinho M, Lin PB, et al. CX3CR1 deficiency aggravates amyloid driven neuronal pathology and cognitive decline in Alzheimer's disease. *Mol Neurodegener*. 2022;17:47.
48. Breese MR, Liu Y. NGSUtils: a software suite for analyzing and manipulating next-generation sequencing datasets. *Bioinformatics*. 2013;29:494-496.
49. Dobin A, Davis CA, Schlesinger F, et al. STAR: ultrafast universal RNA-seq aligner. *Bioinformatics*. 2013;29:15-21.
50. Langmead B, Salzberg SL. Fast gapped-read alignment with Bowtie 2. *Nat Methods*. 2012;9:357-359.
51. Liao Y, Smyth GK, Shi W. featureCounts: an efficient general purpose program for assigning sequence reads to genomic features. *Bioinformatics*. 2014;30:923-930.
52. Robinson MD, McCarthy DJ, Smyth GK. edgeR: a Bioconductor package for differential expression analysis of digital gene expression data. *Bioinformatics*. 2010;26:139-40.
53. Huang DW, Sherman BT, Lempicki RA. Systematic and integrative analysis of large gene lists using DAVID bioinformatics resources. *Nat Protoc*. 2009;4:44-57.
54. Sherman BT, Hao M, Qiu J, et al. DAVID: a web server for functional enrichment analysis and functional annotation of gene lists (2021 update). *Nucleic Acids Res*. 2022;50:W216-W221.
55. Metsalu T, Vilo J. ClustVis: a web tool for visualizing clustering of multivariate data using principal component analysis and heatmap. *Nucleic Acids Res*. 2015;43:W566-W70.
56. Oakley H, Cole SL, Logan S, et al. Intraneuronal β-amyloid aggregates, neurodegeneration, and neuron loss in transgenic mice with five familial Alzheimer's disease mutations: potential factors in amyloid plaque formation. *J Neurosci*. 2006;26:10129-40.
57. Oblak AL, Lin PB, Kotredes KP, et al. Comprehensive evaluation of the 5XFAD mouse model for preclinical testing applications: a MODEL-AD Study. *Front Aging Neurosci*. 2021;13:713726.
58. Peng Q, Malhotra S, Torchia JA, Kerr WG, Coggeshall KM, Humphrey MB. TREM2- and DAP12-dependent activation of PI3K requires DAP10 and is inhibited by SHIP1. *Sci Signal*. 2010;3(122):ra38.
59. Wang S, Sudan R, Peng V, et al. TREM2 drives microglia response to amyloid-β via SYK-dependent and -independent pathways. *Cell*. 2022;185:4153-4169.e19.
60. Wang Y, Ulland TK, Ulrich JD, et al. TREM2-mediated early microglial response limits diffusion and toxicity of amyloid plaques. *J Exp Med*. 2016;213:667.
61. McCray TJ, Bedford LM, Bissel SJ, Lamb BT. Trem2-deficiency aggravates and accelerates age-related myelin degeneration. *Acta Neuropathol Commun*. 2024;12:154.
62. Meilandt WJ, Ngu H, Gogineni A, et al. Trem2 deletion reduces late-stage amyloid plaque accumulation, elevates the abeta42:abeta40 ratio, and exacerbates axonal dystrophy and dendritic spine loss in the PS2APP Alzheimer's mouse model. *J Neurosci*. 2020;40:1956-1974.

SUPPORTING INFORMATION

Additional supporting information can be found online in the Supporting Information section at the end of this article.

How to cite this article: Messenger EJ, Baar SA, Bedford LM, et al. PLCG2 modulates TREM2 expression and signaling in response to Alzheimer's disease pathology. *Alzheimer's Dement*. 2025;21:e70231. https://doi.org/10.1002/alz.70231